A Software Tool for Volume Registration and Atlas-Based Segmentation of Human Fat-Water MRI Data in Longitudinal Studies

A. A. Joshi[1], H. H. Hu[2], M. Goran[3], R. Leahy[2], A. Toga[1], and K. Nayak[2]

[1]Department of Neurology, David Geffen School of Medicine, UCLA, Los Angeles, CA, United States, [2]Ming Hsieh Department of Electrical Engineering, University of Southern California, Los Angeles, [3]Keck School of Medicine, University of Southern California, Los Angeles, CA

INTRODUCTION – Obesity remains a worldwide epidemic in children, adolescents and adults [1]. The accumulation of subcutaneous, visceral, and organ fat have adverse effect on overall health, and increases the risks of heart disease, type 2 diabetes, metabolic disorders, sleep apnea, and certain types of cancer [2-4]. Accurate quantification of the volumes of subcutaneous and visceral adipose tissue depots as well as the degree of fat infiltration in the liver, pancreas, skeletal muscle, and kidneys are important endpoints in determining the efficacy of therapeutic and interventional measures against obesity. The monitoring of changes in adiposity and organ fat during the course of intervention is critical in longitudinal studies, which requires the same subject to be imaged and analyzed at multiple time points. The ability to rapidly determine these desired fat endpoints at each time point would be beneficial to obesity researchers. Previous works have focused primarily on the segmentation and registration of subcutaneous and visceral fat depots [5-8]. In this work, we additionally focus on the organs (liver, pancreas, and kidney). Based on manually segmented labels of adipose tissue depots and organs in each subject at an *initial* time point, we introduce a framework that applies deformable registration of the labels to achieve automated segmentation of the fat depots and organs in the same subject at subsequent time points.

Figure 1. Flow chart of deformation/registration algorithm.

METHODS – MRI exams were performed on a 3T scanner (GE Healthcare) using an eight-channel torso array. Four subjects were recruited to test the deformation/registration algorithm. A 3D SPGR IDEAL-T2* sequence with multi-fat-peak spectral modeling was used [9]. Sixty to seventy axial 5 mm slices from the top of the liver to the iliac crest were acquired in multiple breath-holds. In-plane spatial resolution was 1.5 to 2.5 mm depending on body habitus. Other parameters were: flip angle = 5°, BW = 125 kHz, six echoes, echo train length = 3, echo spacing = 0.8 ms, and rate-2 parallel imaging. Each subject was scanned a second time, after complete repositioning of the coil and the participant on the scanner table. Reconstructed fat, water, and fat fraction images were then utilized for subsequent segmentation and registration.

We used an atlas-based algorithm for image registration with deformable model segmentation (Figure 1). We define the **atlas data set** as taken at one time, and the **target data set** as taken at another time. Labels for adipose tissue depots and organs were first manually segmented in Matlab for all data sets and served as the reference standard. In each subject, we then implemented the algorithm in Insight Toolkit (ITK) using C++ on a designated atlas data set. First, a <u>rigid</u> registration was performed between the atlas and the target to correct for rotations and translations. Second, nonlinear deformations of the organs were performed by using BSpline <u>non-rigid</u> registration. The resultant warping field was then applied to the atlas labels to generate corresponding warped labels for the target data set. To evaluate the accuracy of the warped labels for the target data set, we used the Dice Coefficients **(DC)** [10]. For two label sets A and B, the DC is given by $2|A \cap B|/(|A|+|B|)$, and quantifies the amount of overlap between the two. The DC ranges from 0 to 1, where 1 signifies exact overlap between A and B. In this work, A and B are the warped atlas labels generated by the deformation field and the reference labels generated by manual segmentation for the target data set, respectively.

RESULTS – Figure 2 summarizes results from two subjects. Each panel shows an overlay of labels on a target image. The first column shows labels from the atlas prior to registration; the second column shows warped atlas labels; the third column shows the reference manually segmented labels. Subcutaneous adipose tissue is in yellow; visceral adipose tissue is in pink; liver is shown in blue; kidneys are highlighted in green; and the pancreas in red. Note that in both subjects, the target image is poorly segmented by the default atlas labels, particularly in the visceral adipose tissue depot and kidneys. However, performance is greatly improved after the atlas labels were warped by the deformation algorithm. The degree of overlap between the warped labels and the manually segmented labels are summarized by the DC in Table 1. Based on Table 1, we observed that the target data set was labeled accurately for all adipose tissue depots, the liver, and the kidneys after non-rigid registration, due to their high signal contrast. The lower DC in the pancreas can likely be explained by poor signal contrast in this organ, partial volume effects, and that the organ is small, elongated, and difficult to locate.

atlas labels (no registration) — warped atlas labels (after registration) — manual labels

Figure 2. Overlay of atlas, warped, and reference manual labels on two subjects with different body habitus. The base grayscale images in each row are the same, and are from the **target** data set.

CONCLUSION – We have demonstrated the utility and feasibility of an atlas based registration approach for *intra*-subject segmentation of adipose tissue depots and organs in whole-abdomen MRI. We have shown that manual effort to label different anatomies can be significantly reduced by performing this labeling at an initial time point, and then applying the atlas-based deformation algorithm to automatically label images at remaining time points. We are further investigating the algorithm's potential for *inter*-subject automated segmentation. This is a more challenging task due to the large variations in organ shapes and sizes between normal, overweight, and obese subjects. Work-in-progress include the integration of tetrahedral mesh and active appearance models to address these large inter-subject variations in body habitus

Label Name	DC after <u>Rigid</u> Registration	DC after <u>Non-rigid</u> Registration
Subcutaneous fat	0.71 (0.035)	0.92 (0.017)
Visceral fat	0.56 (0.090)	0.88 (0.028)
Liver	0.46 (0.078)	0.90 (0.031)
Kidneys	0.19 (0.178)	0.89 (0.154)
Pancreas	0.31 (0.154)	0.62 (0.121)

Table 1. Average (standard deviation) Dice Coefficients (DC) across 4 subjects after rigid and non-rigid registration.

REFERENCES – [1] Ogden CL, et al. *JAMA* 2006;295:1549-1555. **[2]** Goran MI, et al. *Am J Clin Nutr* 1999;70:149S-156S. **[3]** Despres JP, et al. *Nature* 2006;444:881-887. **[4]** Bergman RN, et al. *Am J Med* 2007;120:S3-8. **[5]** Kullberg et al. *JMRI* 2009; 30:185-193. **[6]** Demerath EW, et al. *Int J Obesity* 2007; 31:285-291. **[7]** Positano V, et al. *JMRI* 2004;200:684-689. **[8]** Leinhard OD, et al. *ISMRM* 2009:206. **[9]** Yu H, et al. *MRM* 2008, 60:1122-1134. **[10]** C. J. van Rijsbergen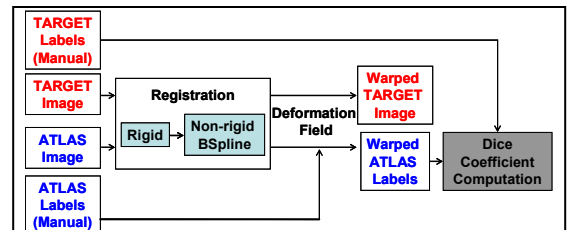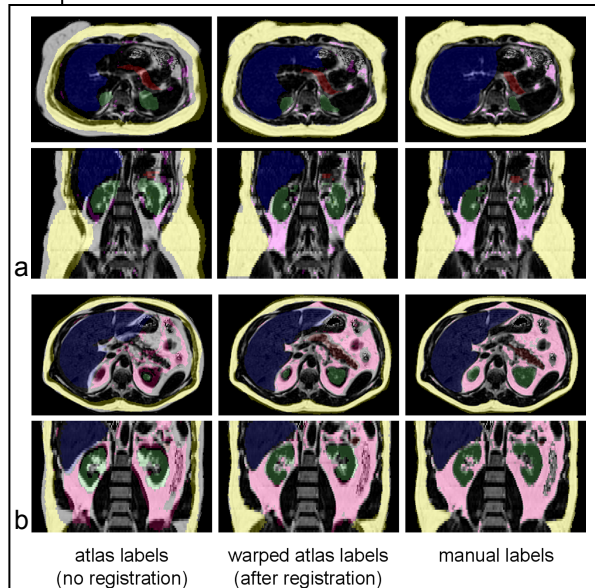 (1979) Information Retrieval (London: Butterworths).